J Fluoresc (2012) 22:1189–1199
DOI 10.1007/s10895-012-1059-8

ORIGINAL PAPER

SYBR Green I: Fluorescence Properties and Interaction with DNA

A. I. Dragan · R. Pavlovic · J. B. McGivney · J. R. Casas-Finet · E. S. Bishop · R. J. Strouse · M. A. Schenerman · C. D. Geddes

Received: 18 March 2012 / Accepted: 9 April 2012 / Published online: 26 April 2012

Abstract In this study, we have investigated the fluorescence properties of SYBR Green I (SG) dye and its interaction with double-stranded DNA (dsDNA). SG/dsDNA complexes were studied using various spectroscopic techniques, including fluorescence resonance energy transfer and time-resolved fluorescence techniques. It is shown that SG quenching in the free state has an intrinsic intramolecular origin; thus, the observed >1,000-fold SG fluorescence enhancement in complex with DNA can be explained by a dampening of its intra-molecular motions. Analysis of the obtained SG/DNA binding isotherms in solutions of different ionic strength and of SG/DNA association in the presence of a DNA minor groove binder, Hoechst 33258, revealed multiple modes of interaction of SG inner groups with DNA. In addition to interaction within the DNA minor groove, both intercalation between base pairs and stabilization of the electrostatic SG/DNA complex contributed to increased SG affinity to double-stranded DNA. We show that both fluorescence and the excited state lifetime of SG dramatically increase in viscous solvents, demonstrating an approximate 200-fold enhancement in 100 % glycerol, compared to water, which also makes SG a prospective fluorescent viscosity probe. A proposed structural model of the SG/DNA complex is compared and discussed with results recently reported for the closely related PicoGreen chromophore.

Keywords Syber Green · Picogreen · Metal-enhanced fluorescence · Fluorescence · Correlation spectroscopy · DNA · Intercalating dyes

Abbreviations

SG	SYBR Green I
PG	PicoGreen
MEF	Metal-Enhanced Fluorescence
FCS	Fluorescence Correlation Spectroscopy
FRET	Fluorescence Resonance Energy Transfer

Introduction

Fluorescence spectroscopy is a powerful technique with utility for studying the dynamic interactions and visualization of macromolecules and macromolecular complexes such as nucleic acids and proteins. The application of fluorescence techniques to various bioanalytical assays is based on the use of different fluorescence probes that can interact with macromolecules and, consequently, sensitize them for spectroscopic studies. Specific fluorophores that effectively interact with nucleic acids (DNA, RNA) significantly

A. I. Dragan · R. Pavlovic
Institute of Fluorescence,
University of Maryland Baltimore County,
701 East Pratt Street,
Baltimore, MD 21202, USA

J. B. McGivney · J. R. Casas-Finet · R. J. Strouse · M. A. Schenerman
MedImmune LLC,
1 MedImmune Way,
Gaithersburg, MD 20878, USA

E. S. Bishop
Cygnus Technologies,
4705 Southport Supply Road,
Southport, NC 28461, USA

C. D. Geddes (✉)
Institute of Fluorescence and Department of Chemistry and Biochemistry, University of Maryland Baltimore County,
701 East Pratt Street,
Baltimore, MD 21202, USA
e-mail: geddes@umbc.edu

increase their brightness upon complex formation. This property makes them useful in various DNA detection assays, in biophysical research of DNA-protein complexes and for chromosome staining. Examples of classical DNA-binding dyes, of which the energetics and mode of interaction with nucleic acids are well studied, include: *ethidium bromide (EB)*, which intercalates between DNA base pairs; *Hoechst 33258*, which binds the DNA minor groove at AT-rich sites; and *acridine orange*, which effectively binds both DNA and RNA. For these chromophores, the enhancement of fluorescence upon binding to nucleic acid usually does not exceed 100-fold. More recently, SYBR Green I (SG) and PicoGreen (PG) have been used in a variety of DNA detection and analysis techniques, due to their ability to dramatically (>1,000-fold) increase brightness upon interaction with double stranded DNA [1–11]. Use of SG and PG has been largely successful despite a lack of detailed knowledge of the spectral properties and nucleic acid binding characteristics of these two dyes.

The structures of both SG and PG were recently determined using a combination of both mass spectroscopy and NMR [11] and are indeed very similar (Fig. 1a, b). Both dyes are used mostly as a stain for nucleic acids in molecular biology applications. It has been demonstrated that, in the presence of dsDNA, the fluorescence of both SG and PG dramatically increases: *i.e.* sensitivity is <10 pg/ml [5]. These properties make SG and PG particularly suited for molecular biology applications including DNA detection in real-time PCR analyses, for registration kinetics of DNA enzymatic digestion both in solution and *in situ* [4] and for chromosome staining and DNA detection assays [12].

Recently, we have shown that the fluorescence of PG in complex with DNA can be significantly enhanced by the presence of silver nanoparticles as compared to free PG in solution. The enhancement of PG fluorescence in the vicinity of metal nanoparticles is due to the metal-enhanced fluorescence (MEF) effect [13]. A similar enhancement due to MEF effect has also been shown for SG in complex with dsDNA (*unpublished results*). The combination of metal nanoparticles with ultra-bright chromophores, such as SG and PG, expands the potential scope of fluorescence applications for these dyes, allowing for exquisitely sensitive DNA detection and quantitation.

In this report, we have analyzed the spectral properties of free SG in solutions of varying viscosity and polarity, aiming to understand and exploit the unique properties of SG. We have also investigated the energetics of the SG/DNA interaction, including a determination of the Gibbs energy of association and its dependence upon ionic strength, and binding site size of SG. Furthermore, we have determined the role of electrostatic forces in SG/DNA complex stabilization and the mode of binding (*e.g.*, intercalation *versus* surface binding; DNA minor groove *versus* DNA major groove binding). The results of this study and proposed model of the SG/DNA complex are discussed, and the results compared to recent studies of the PG chromophore [14].

Materials and Methods

Materials The concentration of ethidium bromide (Sigma Aldrich, St. Louis, Missouri, USA), Hoechst 33258 (Sigma Aldrich), PicoGreen (Invitrogen, Carlsbad, California, USA) and SYBER Green I (Invitrogen) were determined by measuring the optical density of the solutions using the extinction coefficients of E_{480}=5,600 M^{-1} cm^{-1}, E_{245}=46,000 M^{-1} cm^{-1}, E_{495}=70,000 M^{-1} cm^{-1} and 75,000 M^{-1} cm^{-1}, respectively [15]. The chemical structure of SG is shown in Fig. 1a [11]. The IUPAC name for SG is N′,N′-dimethyl-N-[4-[(E)-(3-methyl-1,3-benzothiazol-2-ylidene)methyl]-1-phenylquinolin-1-ium-2-yl]-N-propylpropane-1,3-diamine. The mass of SG is 509.73 g·mol^{-1}.

DNA Samples In this study, we used highly polymeric calf thymus DNA purchased from Sigma Aldrich and a 50 base pair (bp) DNA duplex synthesized by Integrated DNA Technologies (Coralville, Iowa, USA). The single-stranded, complementary, 50 bp oligonucleotides (a portion of Chinese hamster ovary (CHO) *Alu* sequence: 5′-^{1}GAG ATA TGA GCA AAA GAA ACT TGG AAA GGA GGC TGG AGA GAT GGC TCG AG^{50}-3′) were additionally purified by anion exchange FPLC on a Mono-Q column using a linear 0.1 to

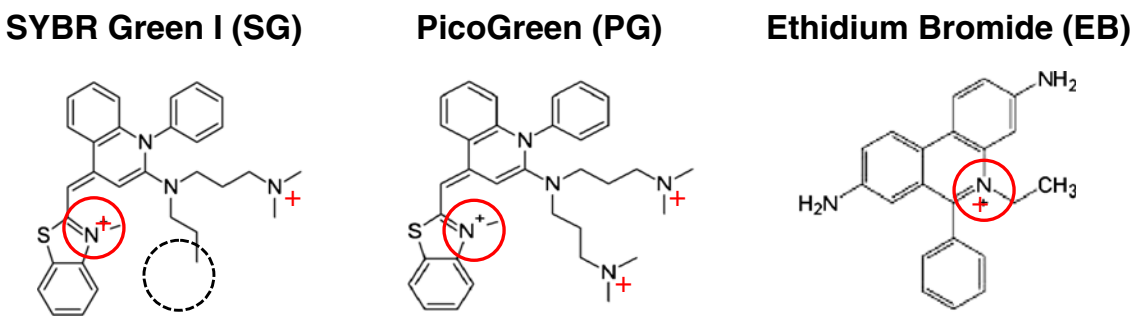

Fig. 1 Molecular structure of SYBR Green I (**left**), PicoGreen (**center**) and Ethidium Bromide (**right**)

1.0 M NaCl gradient in 10 mM Tris–HCl buffer (pH 7.0), 1 mM EDTA, 20 % acetonitrile. The oligonucleotides were precipitated with ethanol, pelleted and air-dried. Concentrations of single-stranded DNA (ssDNA) and double-stranded DNA (dsDNA) were determined from the A_{260} of the nucleotides after complete digestion by phosphodiesterase I (Sigma Aldrich) in 100 mM Tris–HCl (pH 8.0) [16]. The DNA duplex was prepared by mixing the complementary oligonucleotides in equimolar amounts, heating to 70 °C, and then cooling slowly to room temperature. Solutions of dsDNA were prepared for the experiments by extensive dialysis against the required buffer.

Fluorescence and Absorption Measurements Fluorescence and excitation spectra of free SG and SG in complex with DNA were measured on a Cary Eclipse (Varian, Inc., Palo Alto, California, USA) spectrofluorimeter at room temperature. SG was excited at 485 nm and the fluorescence monitored over the wavelength range 490 to 800 nm. A 0.4 cm path-length Suprasil quartz cell (Hellma USA, Inc., Plainview, New York, USA) was used. Absorption spectra of DNA samples (ssDNA and dsDNA) and chromophores (Hoechst and SG) were measured on a Cary (Varian, Inc.) spectrophotomer at room temperature.

Fluorescence Decay Measurements The fluorescence decay functions of SG in both the free state and in complex with dsDNA were measured using a TemPro Fluorescence Lifetime System (Horiba Jobin Yvon, Edison, New Jersey, USA). The reference cell contained colloidal silica; SM-30 LUDOX® solution was used as a control (zero lifetime). Measurements were performed at room temperature. Calculations of SG excited state lifetimes (τ_i) and corresponding amplitudes (A_i) were undertaken using TemPro Fluorescence Lifetime System software (DAS 6). In general, when a fluorescence decay function exhibited more than a single component, the amplitude weighted fluorescence lifetime was calculated:

$$\langle \tau \rangle = \sum_{i=1}^{n} A_i \times \tau_i \tag{1}$$

where n is a number of fluorescence decay components in the total decay function.

Computation of Hoechst-SG Förster Distance The Förster distance (R_o) for fluorescence resonance energy transfer from Hoechst 33258 to SG was calculated using the following equations [17]:

$$R_o = 9.79 \times 10^3 \left(k^2 n^{-4} \phi_D J\right)^{1/6}, \text{Å}, \tag{2}$$

$$J = \int_0^{\infty} F_D(\lambda) \times \varepsilon_A(\lambda) \times \lambda^4 d\lambda \tag{3}$$

where k=2/3 is a factor of the donor and acceptor transition vector's relative orientation, assuming free rotation of the dyes; n=1.333 is the refractive index of the media (water); ϕ_D=0.42 is the quantum yield of Hoechst 33258 in complex with DNA [18]; J is the spectral overlap integral expressing the extent of overlap between the fluorescence spectra of a donor (F_D) and absorption spectra of an acceptor (ε_A). The molar extinction coefficient of SG (ε_{495}=75,000 M^{-1} cm^{-1}) was used in the calculations [11, 18]. Normalized absorption spectra of SG and the corrected fluorescence spectra of Hoechst 33258 in complex with calf thymus DNA (Hoechst/DNA ratio was 0.05 dyes per DNA bp) are shown on Fig. 2.

Analysis of Fluorescence Resonance Energy Transfer (FRET) Data Resonance energy transfer from Hoechst 33258 (donor), a DNA minor groove binder, to the SG chromophore (acceptor) occurs when both dyes sit at close distance to each other along the DNA molecule. In this case, one can observe Förster type quenching, where the fluorescence brightness and excited state lifetime of the donor chromophore decreases. An average distance between the donor and the acceptor can be estimated directly from the fluorescence decay curves (F(t)) using the following analytical equation for 2D model:

$$F(t) = A + B_1 \exp\left[\left(-\frac{t}{\tau_1}\right) - 2\gamma\left(-\frac{t}{\tau_1}\right)^{1/3}\right] \tag{4}$$

where $\gamma = A/A_o$ is a parameter reflecting the efficiency of FRET; A is the acceptor concentration; and A_o is a critical acceptor concentration [17].

Analysis of SG Binding to dsDNA Analysis of the experimental binding data was carried out using the conditional probability model for non-cooperative excluded site binding

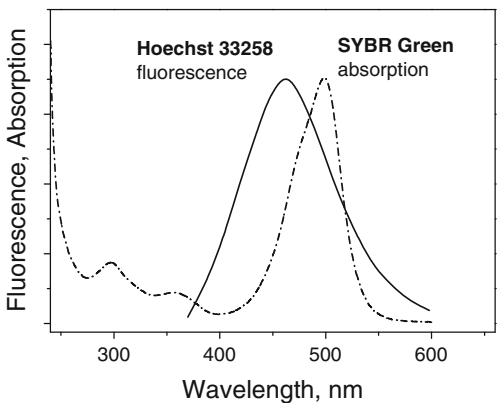

Fig. 2 Normalized absorption spectra of SG (dash lines) and fluorescence spectra of Hoechst 33258 (solid lines). Fluorescence spectra of Hoechst 33258 overlaps with absorption spectra of SG

derived by McGhee and VonHippel [19]. The expression for SG binding to DNA is given by:

$$\nu/L = K_a(1 - n\,\nu)^n/(1 - n\,\nu + \nu)^{(n-1)} \quad (5)$$

where K_a is the intrinsic (observed) association constant; n is the size of the binding site in base pairs, *i.e.* the number of DNA base pairs excluded to another dye by each bound dye molecule.

Results and Discussion

Fluorescence Properties of SG and the Origin of Fluorescence Enhancement Upon Interaction with DNA

Upon binding to dsDNA, the fluorescence of SG is enhanced >1,000-fold (Fig. 3, left). Similar enhancement of fluorescence emission was demonstrated for PG [5, 18], which was used in the recently reported analysis of PG binding to DNA [14].

To elucidate the origin of SG enhancement in complex with DNA, changes in both SG fluorescence emission and decay functions upon binding to dsDNA were determined. The results are shown in Fig. 3. The ratio of fluorescence intensity of SG/DNA complex to free SG is~1,000. Under the same conditions, the fluorescence decay function of SG/DNA is mono-exponential and characterized by lifetime τ= 5.1±0.02 nsec, a value is similar to the value previously measured for the PG/DNA complex – τ=4.4±0.01 nsec [5]. Likewise, the lifetime of free SG is dramatically lower, τ= 3.1±3.0 psec, a value similar to the lifetime of free PG - τ= 3.9±3.0 psec [5]. Results show that the change in fluorescence intensity (F) is nearly proportional to the change in the chromophore lifetime (τ), F~τ, which strongly suggests the dynamic origin of SG quenching in solution. It should be noted that the fluorescence decay function is sensitive to the distribution of chromophore molecule conformers, reflecting the presence of different types of interactions with other molecules. Multi-exponential decay is a reflection of system heterogeneity, while a mono-exponential decay is a manifestation of a homogenous system. Thus, the observed mono-exponential emission decay function of SG/DNA points to a narrow distribution of electronic states for SG in association with DNA and that its mode of interaction with DNA bases is monodisperse and uniform.

Additional information on the origin of SG quenching in solution can be obtained by studying its fluorescent properties in solutions of different viscosity and polarity. Dynamic quenching of SG could be explained by two mechanisms. The external mechanism is bimolecular collisional quenching, which is under diffusional control. The internal mechanism is quenching caused by the inherent flexibility of the molecule, which is independent of diffusion. Screening of the chromophore from the solvent, such as when it is in complex with DNA, can sufficiently decrease the quenching effect and give a rise in the quantum yield. However, this type of quenching is typically small in comparison with the observed magnitude of quenching/enhancement of the dye (~ 1,000-fold) [20]. Furthermore, the total quenching effect, due to bimolecular collisions with small molecular quenchers such as oxygen, is significantly less (<10-fold). Indeed, one cannot rule out this component from observed SG quenching but its contribution is less than 1 %.

In the case of internal quenching, the dissipation of an excited state is under intra-molecular motion control. The frequency and amplitude of segmental motion strongly depends on viscosity. Figure 3 shows SG fluorescence decay profiles in 100 % glycerol, a viscous, low polarity solvent. The fluorescence decay function has several components and the amplitude weighted lifetime is τ_G=0.69± 0.02 nsec, which is about 200-fold greater than in water. However, in 100 % ethanol, which has a polarity lower than water but similar to glycerol, the lifetime of SG is even shorter than in water (data not shown), and below the limit of measurable lifetime range of the time-domain instrument. This suggests that the change in viscosity, but not solvent polarity, is responsible for the dramatic fluorescence changes observed in SG/DNA binding experiments.

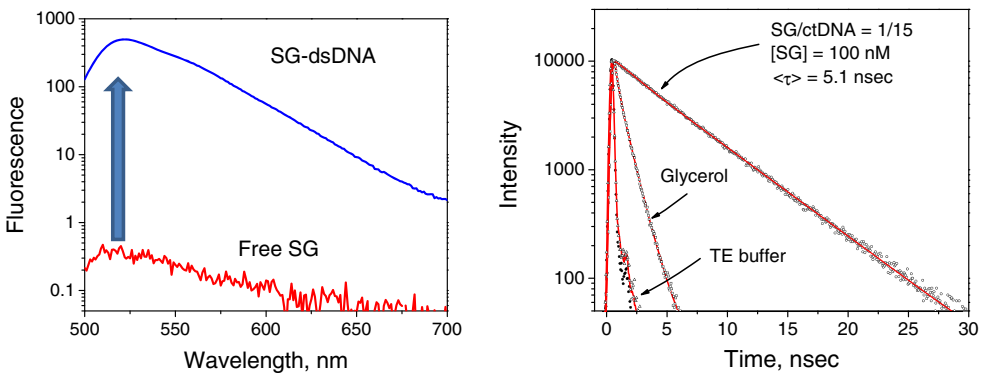

Fig. 3 **(Left)** Fluorescence spectra of SG free in solution and in complex with double-stranded DNA. Observed enhancement of fluorescence >1,000-fold. **(Right)** SG fluorescence decay curves measured in complex with DNA, in 10 glycerol and in water (TE buffer)

The most probable origin of SG fluorescence quenching is from intra-molecular motions that result in perturbation of the thiazole-quinolinium coupled system and the subsequent influence on the effectiveness of the charge transfer event in the excited state. The unimolecular quenching constant, k_q^u, which characterizes the intra-molecular quenching effects, is dependent on viscosity, since viscosity invariably reduces segmental motion in molecules. Because the unimolecular quenching constant is not under diffusional control, but is controlled by the amplitude and frequency of molecule wobbling, quenching efficiency can be ascribed to a charge transfer resulting in radiationless dissipation of excited state. This has been observed for SG; a recent study compared the dependence of the lifetime on viscosity for both PG and SG dyes, and demonstrated that they are very similar [14]. This assumes that the fluorescence properties of SG and PG are determined by their aromatic (thiazole-quinolinium) core, and that there is minimal influence of the arm-like backbone residues.

The sensitivity of SG and PG to viscosity but not solvent polarity makes them particularly intriguing as viscosity probes. It should be noted that there are relatively few known fluorophores characterized as viscosity probes. Of the known viscosity probes, the increase in fluorescence is~ 2-fold in viscous solvents [17]. Moreover, the fact that the structure of an extended arm-like residue has no effect on the fluorescence properties of SG/PG, additional perspectives could be achieved by introducing specific modifications on the chromophore to enable covalent attachment of the dyes to macromolecules (proteins, nucleic acids, etc.) *via* the residue and utilizing them as viscosity probes in a broad range of biomedical studies. It should also be noted that a strong luminescence response of SG upon association with DNA allows for the formation of an extremely bright luminescent complex that can be employed for the analysis of its interaction with DNA, simplifying the numerical fitting procedure of chromophore/DNA binding profiles.

Interactions of SG with dsDNA

The dependence of SG fluorescence upon titration into dsDNA was measured at two ionic strengths (Fig. 4). The fluorescence of SG starts to increase at the very beginning of DNA titration, demonstrating progressive binding of the dye to dsDNA. The additional increase of SG/DNA ratio leads to a decline of the slope and a fluorescence intensity approaching a constant saturation level. The fact that binding of SG to DNA dramatically increases the fluorescence quantum yield (F_{bound}/F_{free}>1000-fold, Fig. 3) when compared to the free dye in solution, implies that the contribution of free dye into total fluorescence signal is negligible (<0.1 %). Therefore, the contribution of free dye in solution can be excluded from analytical consideration, which simplifies the

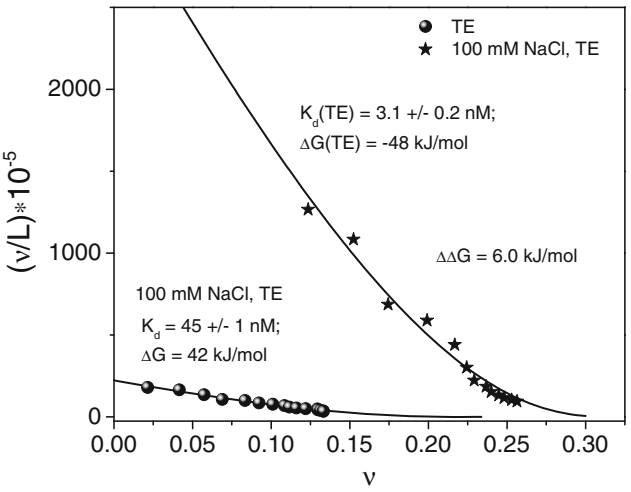

Fig. 4 Binding isotherms of SG to DNA in TE buffer and in 100 mM NaCl, TE, pH 7.6 plotted in Scatchard coordinates and fitted using Eq. (1). *SG* SYBR Green I

binding equation. Accordingly, the fraction of SG dye that is bound to DNA in a course of binding experiments (θ) can be expressed just as:

$$\theta \approx F/F_b, \tag{6}$$

where F is an observed fluorescence intensity of SG and F_b is a fluorescence intensity of 100 % bound SG in solution.

The concentration of free SG in solution at the binding equilibrium can be written as

$$L = (1 - \theta)\, C_{SG} \tag{7}$$

while SG binding density, or the number of bound SG per DNA bp, is

$$\nu = \theta\, C_{SG}/C_{DNA} \tag{8}$$

where C_{SG} and C_{DNA} are the total concentrations of SG and DNA bp in solution, respectively.

In Fig. 4, Scatchard plots of SG binding to calf thymus DNA at two salt concentrations (in TE buffer, pH 7.6 and in 100 mM NaCl, TE buffer, pH 7.6) were generated by applying the conditional probability model for non-cooperative excluded site binding using an analytical expression [5]. The data were fitted using a non-linear least-squares fitting procedure, with K_a and n as fitting parameters. The resulting binding parameters of SG are presented in Table 1, along with the binding parameters of PG and EB to dsDNA [14].

As seen in Table 1, the measured association constants and, thereby, the Gibbs energies of SG binding to DNA at the two ionic strengths were similar to that of PG. However, the size of the SG binding site on DNA is about 1 base pair smaller than it is for the PG/DNA complex [14]. This highlights the structural difference between the SG/DNA and PG/DNA complexes. The only structural difference between

Table 1 DNA binding parameters for SybrGreen (SG), PicoGreen (PG) and Ethidium Bromide (EB)

Dye	TE, pH 7.6			100 mM NaCl, TE, pH 7.6			$\Delta\Delta G_a$, kJ/mol
	K_d, nM	ΔGa, kJ/mol	n, bp	K_d, nM	ΔGa, kJ/mol	n, bp	
SG	3.1±0.2	−47	3.11±0.05	45.0±1.0	−41	4.3±0.06	6
PG*	5.0±0.3	−46	3.76±0.06	45.0±3.0	−41	5.2±0.1	5
EB*	870±25	−34	2.80±0.02	5556±60	−29	2.5±0.02	5

SG and PG is in the number of dimethylamino-groups in two extended propyl-"arms" (Fig. 1: SG has one dimethylamino-group, PG has two dimethylamino-groups), with SG being shorter. Therefore, the difference in binding site size between SG and PG is corroborated in that the extended arms play a role in establishing the length of the dye binding site. This assumption is in agreement with our proposed model for the structure of the PG/DNA complex [14]: the chromophore's arms lie in the minor groove of DNA and, consequently, control the size of the binding site. Additional proof of this mode of SG binding comes from the comparison of the Gibbs energies of interaction of the chromophores listed in Table 1. The Gibbs energy of interaction of both SG and PG is similar but is significantly larger ($\Delta\Delta G \approx 12$ kJ/mol, i.e. ≈ 30 %) than that for EB (Table 1). This is despite the fact that all three of these chromophores form intercalated complexes with DNA [11, 14, 21–23]. The origin of this large excess in binding energy could be derived from an additional set of interactions that SG establishes with DNA; namely, from the interaction between the extended (dimethylamino)-propyl/propyl groups of the either SG or PG and DNA.

Despite their structural differences, both SG and PG have almost equal Gibbs energies of association with DNA (Table 1). The lack of one positively charged dimethyl-amino group in the arm-like residue of SG, as compared to PG, has no effect on the free energy of association to DNA. One can assume that the undetectable contribution of this group to the Gibbs energy is caused by effective enthalpy-entropy compensation upon complex formation. Effective enthalpy-entropy compensation, which maintains the free energy constant, is quite common for DNA binding agents and proteins, especially in the case of minor-groove binders [24–26]. Furthermore, it also suggests that the cationic amino-group probably does not electrostatically interact with DNA phosphates, because this interaction has an entropic nature (enthalpic contribution is close to zero), and should invariably increase the Gibbs energy [25, 27–29].

SG is a positively charged molecule, with a +2 charge at neutral pH (Fig. 1). Electrostatic interactions of SG with negatively charged DNA can play a role in its mode of binding and energy of complex stabilization. Electrostatic interactions are sensitive to the concentration of salt in solution due to the entropic effect of binding [27, 28]. We measured the dissociation constants (K_d) of SG to DNA in solutions with two different salt concentrations. The K_d for SG binding to DNA is 3 nM in TE buffer and 45 nM in TE buffer plus 100 mM NaCl (Table 1). The change in binding parameters as a function of salt concentration is a manifestation of the electrostatic contribution to the Gibbs energy of SG/DNA interaction. Under the conditions tested, the change in Gibbs energy of SG/DNA binding at low salt compared to SG/DNA binding at high salt is $\Delta\Delta G = 5.5$ kJ/mol. This value is in good agreement with the estimated Gibbs energy value for one electrostatic contact (~ 5 kJ/mol) [30], and suggests that only one positively charged group of SG forms an electrostatic contact with DNA upon binding.

The size of the SG binding site (n) on DNA is 3–4 bp, while for PG it is 4–5 bp (Table 1). The binding sites of both dyes are measurably larger than that for the classical intercalator EB. Assuming that SG, PG and EB intercalate into DNA between base pairs, the observed size of the SG and PG binding sites is surprisingly large. On the other hand, the observed differences between the SG/PG and EB binding site sizes could be explained by additional contacts SG/PG along the DNA molecule. This assumption is in agreement with a significantly stronger affinity of SG/PG for DNA compared to that of EB for DNA (Table 1).

Role of the Electrostatic Interactions in the SG/DNA Complex Stabilization

The association constant of the SG/DNA complex was observed to be dependent on the ionic strength of the solution, which indicates that electrostatic forces play an important role in the stability of the SG/DNA complex (as would be expected for a cationic ligand like SG and a polyanion macromolecule such as DNA). Further, the electrostatic interaction of SG with DNA represents the entropic effect of the mixing of the released DNA counterions with ions in bulk solution [28–30]. Therefore, the entropy of their mixing depends on the concentration of the ions in solution. We studied the dependence of the SG/DNA association constant on salt concentration to reveal the contribution of electrostatic and non-electrostatic components to the energy of the SG/DNA interaction (Fig. 5). If Z is the number of DNA phosphate groups that interact with the dye, and $\psi = 0.88$ is

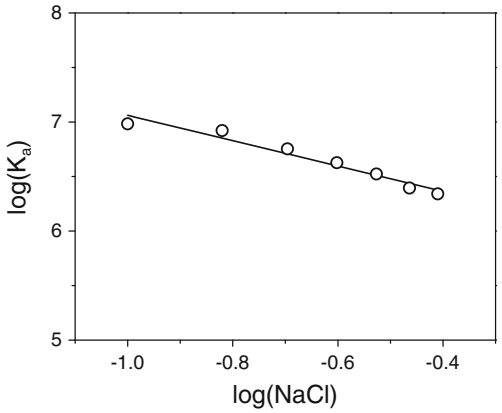

Fig. 5 Dependence of SG/DNA association constant (K_a) upon NaCl concentration in solution. The slope of the dependence log(Ka) *vs.* log (NaCl) is $Z\Psi=1.1\pm0.1$. Number of electrostatic contacts of SG with DNA is $Z=1.2\pm0.1$ ($\Psi=0.88$)

the number of cations (Na^+) per phosphate group that are released upon ligand binding [28, 29], the logarithm of the association constant can be presented as:

$$\log(K) = \log(K_{nel}) - Z\Psi \times \log[NaCl], \quad (8)$$

or, in terms of the Gibbs energy as:

$$\Delta G = \Delta G_{nel} - Z\Psi \times RT \times \ln[NaCl] \quad (9)$$

The first term in Eq. 9 (ΔG_{nel}) results from non-electrostatic interactions between SG and DNA and does not depend on salt concentration. The second term ($\Delta G_{el}=-Z\Psi\times RT\times\ln[NaCl]$) reflects an electrostatic component of the Gibbs energy, which originates from the release of counterions. The electrostatic component of the Gibbs energy is salt-dependent and vanishes at 1 M salt concentration. Thus, at this condition, association of the dye with DNA is stabilized by van der Waals contacts, hydrogen bonding and dehydration effects.

Fitting the data in Fig. 5 to Eq. 8 results in a slope of the function, $\delta\log(K)/\delta[NaCl]=Z\Psi=1.1\pm0.1$ and a y-intercept at $\log[NaCl]=0$, $\log(K_{nel})=5.9\pm0.1$. From the slope, the estimated number of electrostatic contacts between SG and the DNA phosphates is $Z=1.2\pm0.1$, a value that is less than expected for SG (+2 charge at neutral pH). The Gibbs energy of SG/DNA association at 100 mM NaCl can be written in terms of its non-electrostatic and electrostatic components [31] as: $\Delta G=\Delta G_{nel}+\Delta G_{el}=-40$ kJ/mol, where $\Delta G_{nel}=-34$ kJ/mol and $\Delta G_{el}=-6$ kJ/mol. This suggests that a significant part of the SG/DNA affinity originates from non-electrostatic interactions. Hence, the electrostatic component plays a minor role but can be important for maintaining conformational stabilization of the SG/DNA complex. Interestingly, the Gibbs energy of SG/DNA interaction is significantly larger than for EB/DNA ($\Delta G=-30$ kJ/mol, see Table 1), although both dyes have the same number of electrostatic contacts with DNA and, therefore, the same value for the electrostatic Gibbs energy. The magnitude of the difference is $\Delta\Delta G_{nel}^{(SG/EB/DNA)}=\Delta G_{nel}^{(SG/DNA)}-\Delta G_{nel}^{(EB/DNA)}\approx -12$ kJ/mol. A larger binding site size and non-electrostatic Gibbs energy correlate with each other, suggesting that in addition to intercalation, the SG/DNA complex is stabilized by multiple interactions between SG groups and DNA. Probable candidates for such additional contacts with DNA can be the dimethyl-aminopropyl- and propyl-groups of SG, whose length matches well with the observed binding site size. It is worth noting that these elongated arm-like groups have similar structure to the well-known DNA-binding peptides, AT-hooks, that bind DNA in the minor groove [27]. Moreover, the non-electrostatic Gibbs energy of AT-hooks/DNA binding is about −(12–14) kJ/mol [27], which correlates well with the value of $\Delta\Delta G_{nel}^{(SG/EB/DNA)}$.

The slope of the log(K) *versus* log(NaCl) function shows that only one counterion is released upon SG association with DNA. A similar slope was obtained for PG and is also a characteristic of the salt-dependent EB binding to DNA. At a neutral pH, SG has two positive charges, PG has three positive charges while EB has only one positive charge. We infer that the difference in charge in the symmetrical arm-like groups of SG and PG does not influence the slope of salt-dependent dye dissociation and, consequently, the arms do not participate in charge-charge interactions. It can be concluded that only one charge, located in the aromatic moiety of all three dyes, is responsible for the electrostatic interaction with DNA and subsequent counterion release (Fig. 1). In essence, only one possible explanation of the results could be made; namely, the arms of SG and PG lie buried along the DNA groove since the energy of this interaction is most favorable.

SG Binding to DNA: Minor Groove Versus Major Groove

Analysis of SG/DNA association has revealed that the dye forms three different interactions with DNA: intercalation between base pairs, electrostatic interaction and extended contact with the groove of DNA. The last interaction contributes a significant part of the total energy of complex stabilization. To determine if SG interacts with either the major groove or the minor groove of DNA, we studied the competition between SG and Hoechst 33258, a dye that preferentially binds at AT-rich sequences in the minor groove of DNA [32, 33]. Competition between the two dyes for binding would show that SG enters the minor groove while no binding competition would show that SG enters the major groove.

Upon association with DNA, the fluorescence of Hoechst 33258 increases and then approaches a constant level (Fig. 6). Saturation of Hoechst 33258 binding to DNA

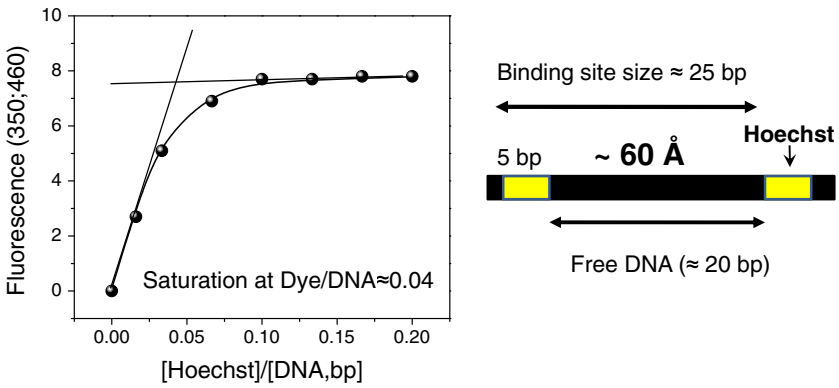

Fig. 6 **(Left)** Binding isotherm of Hoechst 33258 with DNA. Concentration of DNA was 0.5 μM base pairs (bp). **(Right)** Cartoon shows an average distribution of the dye binding sites along highly polymeric DNA

occurs at a ratio of about 0.05 bp^{-1}, which corresponds to a binding site size of approximately 25 bp. However, the physical binding site of Hoechst 33258 on DNA is relatively small, ~5 bp [34]. The discrepancy between two values means that Hoechst 33258 binds to only 20 % of the total DNA, due to its sequence specificity. Subsequently, one can assume that the average distance between the two Hoechst 33258 molecules on DNA is approximately 20 bp (Fig. 6, *right*), a distance that can accept roughly 5–6 molecules of SG.

The change in spectra resulting from titration of a pre-formed Hoechst 33258/DNA complex (dye/DNA=0.1) with SG was measured. The samples were excited at 350 nm, a wavelength at which both dyes absorb light. The fluorescence intensity of Hoechst 33258 starts to decrease at the very beginning of the titration and gradually approaches a minimum of SG/DNA>0.2 (Fig. 7). In contrast, there was a steep increase in fluorescence intensity of SG, reaching a maximum at SG/DNA~0.15, followed by a decrease in intensity that approached a constant level at SG/DNA >0.25 (Fig. 7, *right*). When excited at 472 nm, a wavelength at which only SG absorbs light, the profile of SG fluorescence change is different, showing a gradual increase in fluorescence and then saturation at SG/DNA>0.25. The difference in the profiles of SG fluorescence intensity change at the two excitation wavelengths can be explained by fluorescence resonance energy transfer (FRET) between Hoechst 33258 and SG. There is overlap between fluorescence spectrum of Hoechst 33258 and the absorption spectrum of the SG (Fig. 2), which makes them an appropriate donor-acceptor pair. The calculated Förster radius for the Hoechst 33258-SG donor-acceptor pair is R_0=42 Å (see Material and Methods). It should be noted that the Förster distance value is comparable with an average distance between two Hoechst 33258 molecules on DNA (20 bp or 68 Å) (Fig. 6, *right*). Consequently, during the initial phase of the titration of the pre-formed Hoechst 33258/DNA complex, binding of SG to free DNA sites promptly causes FRET. At the onset of the titration, SG readily binds free DNA in-between Hoechst 33258 bound sites in the Hoechst 33258/DNA complex, since SG does not show a preference for DNA sequence. Energy transfer from Hoechst 33258 to SG effectively quenches Hoechst 33258 fluorescence, with a concomitant increases in SG fluorescence, even when competition between the two dyes is negligible. This explains the steep decrease in Hoechst 33258 fluorescence even at low SG/DNA ratios (Fig. 7, *right*). Under these conditions, there are many free DNA sites and SG does not compete with Hoechst 33258 for binding. However, after saturation of unoccupied DNA sites, SG starts to compete for Hoechst 33258-bound DNA sites. The release of bound Hoechst 33258 from

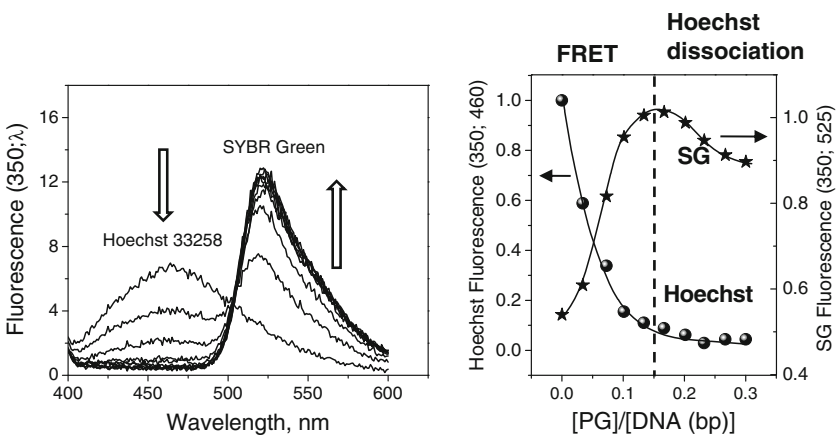

Fig. 7 **(Left)** Changes of Hoechst 33258 and SG spectra upon titration of the DNA/Hoechst 33258 complex (Hoechst 33258/DNA=0.1) with SG. The SG/DNA(bp) ratio increases in equal steps from 0 to 0.3. **(Right)** Dependence of fluorescence intensity of SG and Hoechst 33258 upon titration of Hoechst 33258/DNA complex (Dye/DNA=0.1) with SG. *SG* SYBR Green fluorophore

DNA into bulk solution as a result of competition dramatically increases the distance between donors and acceptors. Therefore, FRET becomes negligible, ultimately leading to a decrease in observed SG fluorescence intensity during excitation at 350 nm. It should be noted that free Hoechst 33258 has a significantly lower quantum yield in solution (Q_{free}=0.015) compared to in complex with DNA (Q_{bound}= 0.42) [18]. Therefore, both the resonance energy transfer to SG and its release from DNA cause a decrease in Hoechst 33258 brightness (Fig. 7) and explains the observed fluorescence quenching in the SG titrations of the Hoechst 33258/DNA complex. A proposed mechanism of the competition between SG and Hoechst 33258 for binding to the minor groove of DNA is shown in Fig. 8.

To gain additional insight into the competition of SG and Hoechst 33258 for DNA binding sites, time-resolved fluorescence decay curves of Hoechst 33258 were analyzed at different ratios of SG/DNA (Fig. 9). Addition of SG to the Hoechst 33258/DNA complex steeply increases the rate of fluorescence decay, due Förster quenching of the donor. At large SG/DNA ratios, the Hoechst 33258 fluorescence decay rate approaches the rate observed for free Hoechst 33258, in support of the dissociation of Hoechst 33258 from DNA (Fig. 9).

An average distance between FRET donor and acceptor can be estimated directly from the Hoechst 33258 fluorescence decay curves at low SG/DNA ratios, when Hoechst 33258 is still associated with DNA, using Eq. (4). From this information, the geometry of each chromophore on DNA can be inferred. Figure 10 (*left*) shows the change in donor-acceptor distance, R_{DA}, upon increased SG/DNA ratio. It is noted that at a low density of SG (SG/DNA~0.03 bp^{-1}), the estimated R_{DA} is 12–13 bp, which corresponds to the approximate distance between two neighbor Hoechst 33258 molecules (Fig. 6, *right*). This result demonstrates free distribution of SG along the DNA. However, upon an increase of SG density, R_{DA} approaches 10 bp at SG/DNA= 0.14 bp^{-1}. This reflects the change in the distribution of R_{DA} distances between SG and Hoechst 33258 and in the orientation of their transition dipole moments. Thus, maximal FRET occurs at R_{DA}≈10 bp or when both SG and Hoechst 33258 are on one face of DNA (Fig. 10). This suggests that the transition dipole moments of the donor and acceptor are in the most favorable orientation; namely, that both molecules are nearly co-linear. In fact, the dipole moments of Hoechst 33258 and SG are oriented along the long axis of the dyes [17, 35] and can be in a favorable orientation for FRET when Hoechst 33258 lies in the minor groove and the SG aromatic core is intercalated between base pairs in the DNA minor groove. In essence, the competition between SG and Hoechst 33258 for association with DNA strongly suggests that upon binding, SG enters the

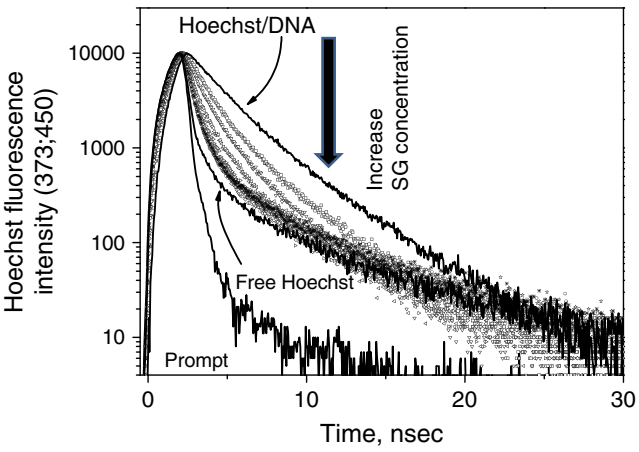

Fig. 9 Time resolved fluorescence decay functions of Hoechst 33258 in complex with DNA (Dye/DNA (bp)=1:10) and upon titration of the complex with SG. Upon titration the ratio of SG/DNA (bp) was changed from 0 to 0.3

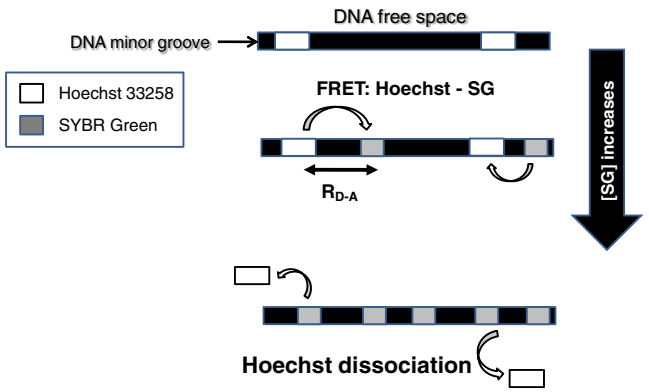

Fig. 8 Cartoon showing the complex process of competition between SG and Hoechst 33258 for binding to the minor groove of DNA

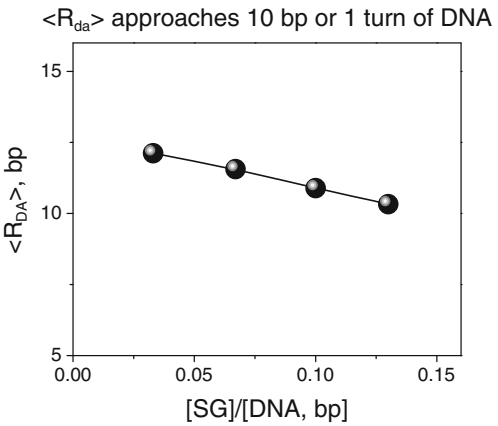

Fig. 10 Average SG (donor)-Hoechst 33258 (acceptor) distances, R_{DA}, calculated from fluorescence decay curves measured at different SG/DNA ratio ([Hoechst 33258]/[DNA, bp]=0.1), shown in Figure 6. Analysis was undertaken using Eq. (1). Maximal FRET between Hoechst 33258 and SG occurs at a distance of≈10–12 bp, i.e. ~1 turn of DNA

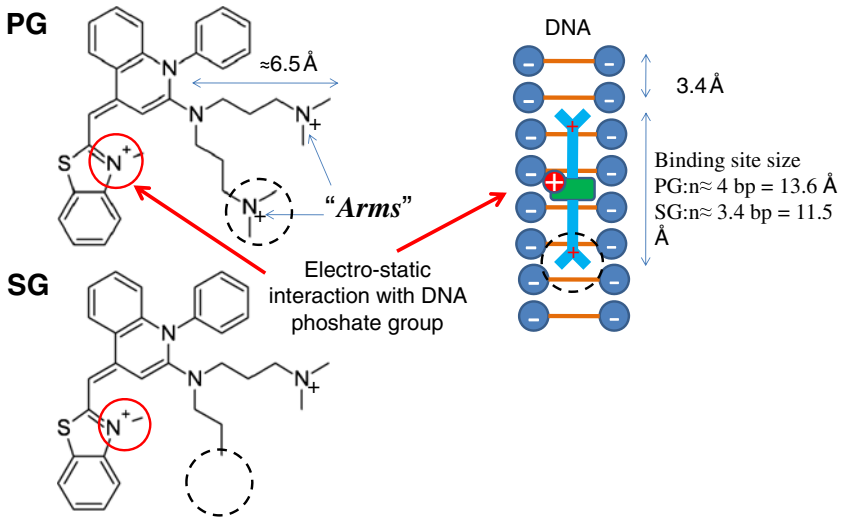

Fig. 11 **(Left)** Structural elements of the SG and PG molecules responsible for the different interactions with DNA; **(Right)** Model of the SG/DNA complex. SG has shorter 'arm' than PG, thus its binding site size is shorter, ~ ½ bp (2 Å; see Table 1)

DNA minor groove, intercalates, and extends its arm-like propyl groups along the groove.

Conclusions

The results of this study demonstrate that the fluorescent properties of SG, such as quantum yield and excited state lifetime, are underpinned by inner segmental motion of the molecule. This explains the dynamic origin of SG fluorescence enhancement/quenching upon association/dissociation from DNA. Intra-molecular flexibility has been shown to strongly depend on the viscosity of the solution, resulting in almost 200-fold increase of SG fluorescence quantum yield and lifetime in viscous solutions. PG has similar properties, as has been recently demonstrated [14].

We have shown that the spectral properties of the fluorescent aromatic core of SG are relatively insensitive to the presence/absence of the dimethylamino-group located in the elongated propyl chain. It may therefore be possible to modify the chromophore for DNA binding with little or no change observed in the fluorescent signals.

We propose a model for SG/DNA complex formation (Fig. 11), which is based on analysis of SG interactions with dsDNA, provided in this study. The main features of the proposed model are similar to the model recently proposed by us for PG/DNA complex [14]. The SG molecule (Fig. 11, *left*) contains phenyl-quinilinium and benzo-thiazole aromatic systems and dimethylaminopropyl and propyl elongated chains. Each of these structural elements contributes to the energy of SG/DNA complex formation. The aromatic rings of SG intercalate into DNA, an interaction that is energetically favorable [18]. The narrow fit of the aromatic group between base pairs coupled with van der Waals interactions with bases significantly dampens internal motion of SG. Additional SG molecular rigidity comes from electrostatic interactions between SG and DNA. As we have shown, the SG/DNA complex is stabilized by a charge-charge interaction formed by positively charged thiazole group and phosphates from the DNA backbone. Intercalation and columbic interaction effectively immobilize the quinilinium-thiazole system in a favorable conformational state, which is characterized by a dramatic enhancement of SG fluorescence and a proportional increase of lifetime and mono-exponential fluorescence decay.

As part of the characterization of the DNA binding mechanism of SG, we first demonstrated that SG binds in the minor groove of DNA minor groove by analyzing the competition between SG and a known minor groove binder (Hoechst 33258) for DNA. SG effectively removes Hoechst 33258 from the complex. Secondly, we have shown that the positively charged amino-group of the elongated arm of SG does not form electrostatic contacts with DNA phosphates. Therefore, we propose that the arm buried on the bottom of the minor groove and its interactions within groove are energetically more favorable than columbic contact with DNA phosphate groups. We have estimated that the energetic contribution (10 kJ/mol) of the arm to the Gibbs energy of SG/DNA association is significant: almost 30 % from the total binding energy. Thirdly, the size of SG/DNA binding site is in average 3.5 base pairs (~ 11.5 Å), which is significantly longer than it might be expected for intercalation. However, this distance is comparable to the length of SG's arms in an extended conformation (Fig. 11, *left*) and also to PG, which has longer arms, and, therefore, a longer binding site size on DNA. Thus, we suggest that the SG binding site size is controlled by the arms, which extend along the minor groove for approximately 3–4 base pairs.

Acknowledgments The authors would like to thank MedImmune for financial support. Support from the Institute of Fluorescence, Department of Chemistry and Biochemistry and UMBC is also gratefully acknowledged.

References

1. Ahn SJ, Costa J, Emanuel JR (1996) PicoGreen quantitation of DNA: effective evaluation of samples pre- or post-PCR (vol 24, pg 2623, 1996). Nucleic Acids Res 24:3282
2. Becker A, Reith A, Napiwotzki J, Kadenbach B (1996) A quantitative method of determining initial amounts of DNA by polymerase chain reaction cycle titration using digital imaging and a novel DNA stain. Anal Biochem 237:204–207
3. Blaheta RA, Kronenberger B, Woitaschek D, Weber S, Scholz M, Schuldes H, Encke A, Markus BH (1998) Development of an ultrasensitive in vitro assay to monitor growth of primary cell cultures with reduced mitotic activity. J Immunol Methods 211:159–169
4. Choi SJ, Szoka FC (2000) Fluorometric determination of deoxyribonuclease I activity with PicoGreen. Anal Biochem 281:95–97
5. Dragan AI, Bishop ES, Casas-Finet JR, Strouse RJ, Schenerman MA, Geddes CD (2010) Metal-enhanced PicoGreen fluorescence: application for double-stranded DNA quantification. Anal Biochem 396:8–12
6. Murakami P, McCaman MT (1999) Quantitation of adenovirus DNA and virus particles with the PicoGreen fluorescent dye. Anal Biochem 274:283–288
7. Noothi SK, Kombrabail M, Rao BJ, Krishnamoorthy G (2009) Fluorescence characterization of the structural heterogeneity of polytene chromosomes. J Fluoresc
8. Noothi SK, Kombrabail M, Kundu TK, Krishnamoorthy G, Rao BJ (2009) Enhanced DNA dynamics due to cationic reagents, topological states of dsDNA and high mobility group box 1 as probed by PicoGreen. FEBS J 276:541–551
9. Schneeberger C, Speiser P, Kury F, Zeillinger R (1995) Quantitative detection of reverse transcriptase-pcr products by means of a novel and sensitive DNA stain. PCR Methods Appl 4:234–238
10. Singer VL, Jones LJ, Yue ST, Haugland RP (1997) Characterization of PicoGreen reagent and development of a fluorescence-based solution assay for double-stranded DNA quantitation. Anal Biochem 249:228–238
11. Zipper H, Brunner H, Bernhagen J, Vitzthum F (2004) Investigations on DNA intercalation and surface binding by SYBR Green I, its structure determination and methodological implications. Nucleic Acids Res 32:e103
12. Ikeda Y, Iwakiri S, Yoshimori T (2009) Development and characterization of a novel host cell DNA assay using ultra-sensitive fluorescent nucleic acid stain "PicoGreen". J Pharm Biomed Anal 49:997–1002
13. Geddes CD, Lakowicz JR (2002) Metal-enhanced fluorescence. J Fluoresc 12:121–129
14. Dragan AI, Casas-Finet JR, Bishop ES, Strouse RJ, Schenerman MA, Geddes CD (2010) Characterization of PicoGreen interaction with dsDNA and the origin of its fluorescence enhancement upon binding. Biophys J 99:3010–3019
15. Singer VL, Jones LJ, Yue ST, Haugland RP (1997) Characterization of PicoGreen reagent and development of a fluorescence-based solution assay for double-stranded DNA quantitation. Anal Biochem 249:228–238
16. Dragan AI, Carrillo R, Gerasimova TI, Privalov PL (2008) Assembling the human IFN-beta enhanceosome in solution. J Mol Biol 384:335–348
17. Lakowicz JR (2006) Principles of fluorescence spectroscopy. Springer Science + Business Media, LLC, New York
18. Cosa G, Focsaneanu KS, McLean JR, McNamee JP, Scaiano JC (2001) Photophysical properties of fluorescent DNA-dyes bound to single- and double-stranded DNA in aqueous buffered solution. Photochem Photobiol 73:585–599
19. McGhee JD, von Hippel PH (1974) Theoretical aspects of DNA-protein interactions: co-operative and non-co-operative binding of large ligands to a one-dimensional homogeneous lattice. J Mol Biol 86:469–489
20. Lakowicz JR, Weber G (1973) Quenching of fluorescence by oxygen. A probe for structural fluctuations in macromolecules. Biochemistry 12:4161–4170
21. Le Pecq JB, Paoletti CA (1967) A fluorescent complex between ethidium bromide and nucleic acids: physical-chemical characterization. J Mol Biol 27:87–106
22. Morgan AR, Lee JS, Pulleyblank DE, Murray NL, Evans DH (1979) Review: ethidium fluorescence assays. Part 1. Physicochemical studies. Nucleic Acids Res 7:547–569
23. Olmsted J III, Kearns DR (1977) Mechanism of ethidium bromide fluorescence enhancement on binding to nucleic acids. Biochemistry 16:3647–3654
24. Crane-Robinson C, Dragan AI, Privalov PL (2006) The extended arms of DNA-binding domains: a tale of tails. Trends Biochem Sci 31:547–552
25. Dragan AI, Read CM, Makeyeva EN, Milgotina EI, Churchill ME, Crane-Robinson C, Privalov PL (2004) DNA binding and bending by HMG boxes: energetic determinants of specificity. J Mol Biol 343:371–393
26. Privalov PL, Dragan AI, Crane-Robinson C, Breslauer KJ, Remeta DP, Minetti CA (2007) What drives proteins into the major or minor grooves of DNA? J Mol Biol 365:1–9
27. Dragan AI, Liggins JR, Crane-Robinson C, Privalov PL (2003) The energetics of specific binding of AT-hooks from HMGA1 to target DNA. J Mol Biol 327:393–411
28. Record MT Jr, Anderson CF, Lohman TM (1978) Thermodynamic analysis of ion effects on the binding and conformational equilibria of proteins and nucleic acids: the roles of ion association or release, screening, and ion effects on water activity. Q Rev Biophys 11:103–178
29. Record MT Jr, Zhang W, Anderson CF (1998) Analysis of effects of salts and uncharged solutes on protein and nucleic acid equilibria and processes: a practical guide to recognizing and interpreting polyelectrolyte effects, Hofmeister effects, and osmotic effects of salts. Adv Protein Chem 51:281–353
30. Manning GS (1978) The molecular theory of polyelectrolyte solutions with applications to the electrostatic properties of polynucleotides. Q Rev Biophys 11:179–246
31. Privalov PL, Dragan AI, Crane-Robinson C (2011) Interpreting protein/DNA interactions: distinguishing specific from non-specific and electrostatic from non-electrostatic components. Nucleic Acids Res. Feb 8, doi:10.1093/nar/gkq984
32. Haq I, Ladbury JE, Chowdhry BZ, Jenkins TC, Chaires JB (1997) Specific binding of hoechst 33258 to the d(CGCAAATTTGCG)2 duplex: calorimetric and spectroscopic studies. J Mol Biol 271:244–257
33. Utsuno K, Maeda Y, Tsuboi M (1999) How and how much can Hoechst 33258 cause unwinding in a DNA duplex? Chem Pharm Bull(Tokyo) 47:1363–1368
34. Pjura PE, Grzeskowiak K, Dickerson RE (1987) Binding of Hoechst 33258 to the minor groove of B-DNA. J Mol Biol 197:257–271
35. Carlsson C, Larsson A, Jonsson M, Albinsson B, Norden B (1994) Optical and photophysical properties of the oxazole yellow DNA probes Yo and YoYo. J Phys Chem 98:10313–10321